JOURNAL OF GEOPHYSICAL RESEARCH, VOL. 89, NO. A2, PAGES 883–895, FEBRUARY 1, 1984

Generation of Auroral Kilometric and Z Mode Radiation by the Cyclotron Maser Mechanism

N. OMIDI

Department of Physics and Astronomy, University of Iowa

C. S. WU

Institute for Physical Science and Technology, University of Maryland

D. A. GURNETT

Department of Physics and Astronomy, University of Iowa

The relativistic Doppler-shifted cyclotron resonance condition for electromagnetic wave interactions with a plasma is studied. The results indicate that the resonance condition defines an ellipse in velocity space when the product of the index of refraction and cosine of the wave normal angle is less than or equal to 1 and that it defines a partial ellipse when the product is larger than 1. It is also shown that waves with frequencies greater than the gyrofrequency (or its harmonic for higher harmonic resonances) can only resonate with particles moving in the same direction along the magnetic field, while waves with frequencies less than the gyrofrequency (or its harmonic) resonate with particles moving in both directions along the magnetic field. Growth rates for the terrestrial auroral kilometric and Z mode radiation have been calculated by using the relativistic resonance condition and the electron pitch angle distribution measured by the S3-3 satellite in the auroral zone region. In the case of auroral kilometric radiation, it is shown that both the upgoing and the downgoing electrons are unstable and can give rise to the growth of auroral kilometric radiation, although growth due to the downgoing electrons is limited to a much narrower frequency band. The magnitudes of the growth rates for both the upgoing and the downgoing auroral kilometric radiation are comparable and they indicate that the path lengths required to account for the observed intensities of auroral kilometric radiation are of the order of a few hundred kilometers, which is probably too large. Therefore in order for cyclotron maser instability to remain a viable mechanism for the generation of auroral kilometric radiation, it is essential to either have steeper slopes $(\partial F/\partial v_\perp)$ in the loss cone or reflections to increase the path length. The growth rate calculations for the Z mode radiation show that for wave frequencies just below the gyrofrequency and wave normal angles at or near 90°, the electron distribution is unstable and the growth rates are large enough to account for the observed intensities. The fact that Z mode waves with frequencies smaller than the gyrofrequency are amplified can explain the DE 1 observations of Z mode radiation which indicate no radiation exists above the local electron gyrofrequency.

1. INTRODUCTION

The auroral kilometric and the broadband Z mode radiation are two of the three principal types of auroral plasma wave emissions observed by the polar orbiting DE 1 spacecraft [*Gurnett et al.*, 1983]. Since auroral kilometric radiation (AKR) has been extensively studied in the past several years, it is well known that AKR is generated in the high-latitude auroral regions in association with inverted-V electron precipitation regions [*Gurnett*, 1978; *Kaiser and Stone*, 1975; *Kurth et al.*, 1975; *Green et al.*, 1979; *Benson and Calvert*, 1979]. It is also widely believed that while AKR consists of both right-hand and left-hand polarized radiation, the most intense and dominant component of this radiation is generated in the *R-X* mode [*Gurnett and Green*, 1978; *Kaiser et al.*, 1978; *Benson and Calvert*, 1979; *Shawhan and Gurnett*, 1982]. Since 1974 a number of theories have been proposed to explain the generation of AKR. Among the early theories only *Melrose* [1976] predicted right-hand polarized *R-X* mode. He proposed that AKR is generated by the precipitating electrons with a thermal anisotropy. Later, *Wu and Lee* [1979] suggested that mildly relativistic electrons with a loss cone distribution in the auroral zone can give rise to growth of kilometric radiation. These authors stressed the importance of the relativistic effect on the Doppler-shifted cyclotron resonance. Recently, in a number of papers [*Omidi and Gurnett*, 1982; *Wu et al.*, 1982; *Melrose et al.*, 1982; *Dusenbery and Lyons*, 1982; *Hewitt et al.*, 1982] the idea of loss cone instability as the amplification mechanism for AKR has been given further support by comparisons with electron distribution functions measured in the auroral regions.

In the paper by *Omidi and Gurnett* [1982] the relativistic Doppler-shifted cyclotron resonance condition for the free space *R-X* mode was extensively studied. By using the electron distribution in velocity space measured by the S3-3 satellite in the auroral zone region, they calculated the growth rates of AKR and showed that the loss cone region of the distribution is unstable. In the present paper we generalize the discussion of the relativistic resonance condition to any mode of propagation and show that the resonance condition exhibits a variety of interesting features depending upon the values of $Y \equiv nf_g/f$ and $N \cos\theta$, where n is the harmonic number, f_g is the cyclotron frequency, f is the wave frequency, N is the index of refraction, and θ is the wave normal angle.

By using a more accurate expression for the growth rate ω_i than that used in *Omidi and Gurnett* [1982], we show that near

Paper number 3A1684.
0148-0227/84/003A-1684$05.00

the cutoff, where N goes to zero, the previous growth rates were overestimated by more than 1 order of magnitude. However, at higher frequencies the difference between the reported growth rates and the newly calculated ones is not as large. In addition to the calculation of ω_i for upgoing particles, the growth and damping rates due to downgoing electrons which exhibit a "holelike" feature in their pitch angle distribution have also been computed. It was demonstrated by *Omidi and Gurnett* [1982] that for upgoing waves, the frequency region for which cyclotron resonance interaction is possible is usually divided into three separate bands, two of which correspond to positive ω_i and the middle one of which corresponds to damping. This general feature was explained by noting that in the first and the third regions the corresponding resonance ellipses lie mostly or completely in the loss cone region of the distribution, while the ellipses corresponding to the second (damping) region lie mostly outside of the loss cone. However, in the case of waves traveling downward, it will be shown that only two bands exist; one is a narrow band with positive ω_i just above the cutoff frequency ($f_R = 0$), and the second one is a much wider band with negative values of ω_i. This characteristic is explained by noting that the "holelike" feature in the downgoing side of the electron distribution is not as big as the loss cone region, i.e., the free-energy source in the downgoing side of the electron distribution is limited to lower energy electrons. Therefore higher frequency waves which resonate with more energetic electrons cannot be amplified.

Unlike AKR, which has been extensively studied for several years, little is known about the broadband Z mode radiation which is found in the low-density plasma over the high-latitude auroral and polar regions. For example, due to lack of observation and data, the source region has not been exactly located. The DE-1 spacecraft launched in 1981 is now providing new information on Z mode radiation at high altitudes over the auroral regions. These recent measurements have shown that Z mode radiation is not observed between f_g and the upper hybrid resonance frequency f_{UHR} and that it is most intense right below the gyrofrequency. Observations have also indicated that this radiation propagates nearly perpendicular to the geomagnetic field **B**.

Obviously, lack of data and information on the source region has been a limiting factor in explaining the generation mechanism of the Z mode radiation. However, it had been previously suggested that the Z mode could be produced by auroral electron beams [*Taylor and Shawhan*, 1974; *Kaufman et al.*, 1978; *Maggs and Lotko*, 1981]. In this paper, by using the relativistic cyclotron resonance condition and the electron distribution measured by the S3-3 satellite, we demonstrate that Z mode waves with f near and below f_g and $\theta \sim 90°$ can resonate with electrons in the loss cone and the "hole" region of the distribution function. Results of growth rate calculations show that the distribution function is indeed unstable and that growth rates are high enough to account for the observed intensities of the Z mode radiation. Since the above conditions on f and θ are evidently consistent with the observations, the cyclotron instability seems to be a viable mechanism for the generation of the broadband Z mode radiation.

2. General Comments on the Relativistic Cyclotron Resonance

It is well known that in order for a wave with angular frequency ω and wave normal angle θ to resonate relativistically with electrons with angular gyrofrequency ω_g and

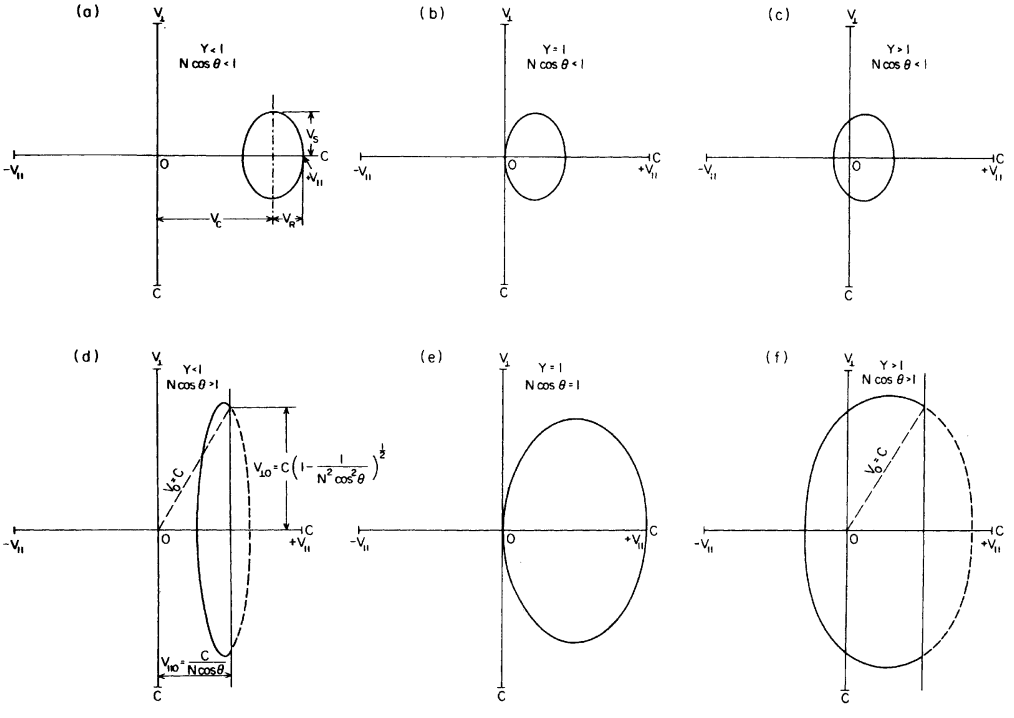

Fig. 1. Six resonance ellipses corresponding to different values of Y and $N_{\|}$. The portion of the ellipse shown by broken line does not correspond to resonance. The resonance ellipse goes through $v_{\|} = c$ whenever $N_{\|} = 1$.

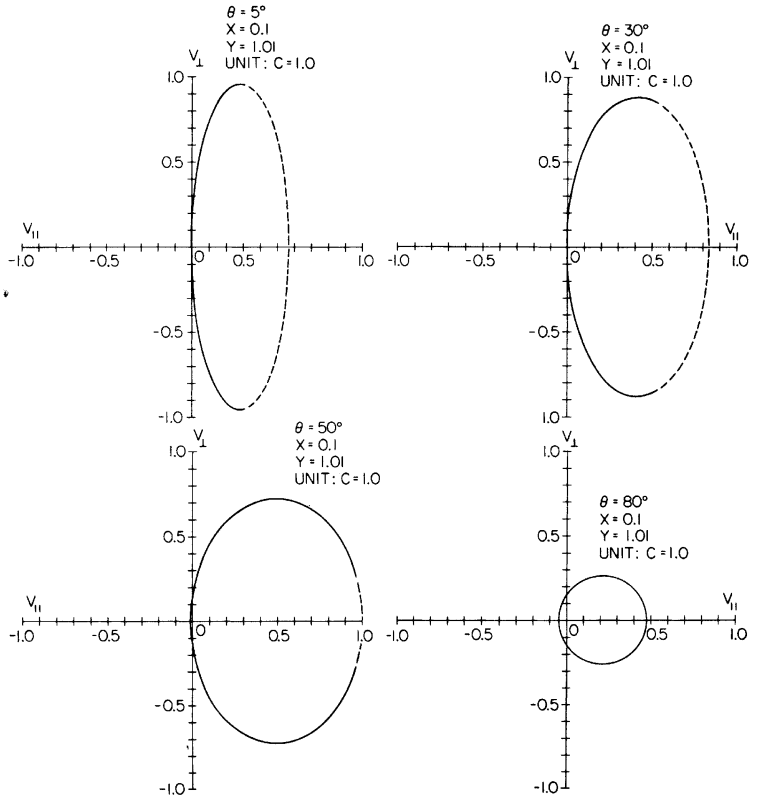

Fig. 2. Four resonance ellipses for the Z mode. As θ increases, the eccentricity decreases and a larger portion of the ellipse corresponds to resonance.

velocity $v_{\|}$ along a magnetic field line, the following condition must be satisfied:

$$\omega - kv_{\|} \cos \theta = (n\omega_g)/\gamma \tag{1a}$$

where $n > 1$ indicates resonance at harmonics of ω_g, k is the wave number, $\gamma \equiv (1 - v^2/c^2)^{-1/2}$, v is electron velocity, and c is the speed of light. Substituting $N\omega/c$ for k and dividing both sides of equation (1a) by ω, one obtains

$$1 - N \cos \theta(v_{\|}/c) = Y(1 - v^2/c^2)^{1/2} \tag{1b}$$

squaring both sides of equation (1) results in an equation for an ellipse [*Omidi and Gurnett*, 1982; *Wu et al.*, 1982; *Melrose et al.*, 1982; *Dusenbery and Lyons*, 1982]. This ellipse has a center at $V_c = B/A$, semiminor axis $V_R = D/A$, and semimajor axis $V_S = D/Y$ (Figure 1a), where

$$A = (Y^2 + N^2 \cos^2 \theta)^{1/2} \tag{2a}$$

$$B = (cN \cos \theta)/A \tag{2b}$$

and

$$D^2 = c^2(Y^2 - 1) + B^2 \tag{2c}$$

Rather than analyzing the resonance condition for each specific mode of propagation, one can study how the parameters Y and $N_{\|} = N \cos \theta$ can affect the size and position of the resonance ellipse. Once this is done, it will be a matter of knowing the values of Y and $N_{\|}$ in a specific mode, and an overall view of the resonance condition will be at hand. Note that Y and $N_{\|}$ completely determine the resonance ellipse.

As can be seen in Figure 1, the semiminor axis of the resonance ellipse lies on the $v_{\|}$ axis. From the definitions of V_C and V_R it is clear that if $B > D$, then the resonance ellipse lies entirely in the region $v_{\|} > 0$, i.e., all resonance parallel velocities will be positive (Figures 1a, 1d). Note that positive $v_{\|}$ corresponds to a direction along **B** for which $k_{\|} \equiv k \cos \theta$ has a positive value, i.e., it is the wave vector **k** that determines which side of the distribution corresponds to positive $v_{\|}$. Similarly, for $B = D$ the ellipse will go through the origin (Figures 1b, 1e), and for $B < D$ the resonance ellipse encircles the origin (Figures 1c, 1f). From equation (2c) it is evident that $D > B$ if $Y > 1$, $D = B$ if $Y = 1$, and $D < B$ if $Y < 1$, which means that for $Y < 1$ only particles with positive $v_{\|}$ can resonate with waves, but for $Y > 1$ particles with both positive and negative parallel velocities resonate with waves. Note that this result can only be obtained if the relativistic resonance condition is used, i.e., if γ is set equal to 1 for low-energy electrons in equation (1), then depending upon the value of Y only particles with $v_{\|} > 0$ or $v_{\|} < 0$, but not both, can resonate with the waves.

In order to study the role of $N_{\|}$ it should be noted that, since the equation of the resonance ellipse is obtained by squaring both sides of equation (1), it is possible that this equation may have false roots [*Melrose et al.*, 1982]. Since the right-hand side of equation (1b) is always positive, the left-hand side must also be positive, and any $v_{\|}$ for which the left-hand side is negative is a false root. Clearly, for $N_{\|} < 1$, all parallel velocities corresponding to the resonance ellipse are acceptable roots because the term $N_{\|}v_{\|}/c$ is always less than 1, and therefore the left-hand side of equation (1b) is always positive (Figures 1a, 1b, 1c). On the other hand, for $N_{\|} > 1$ the

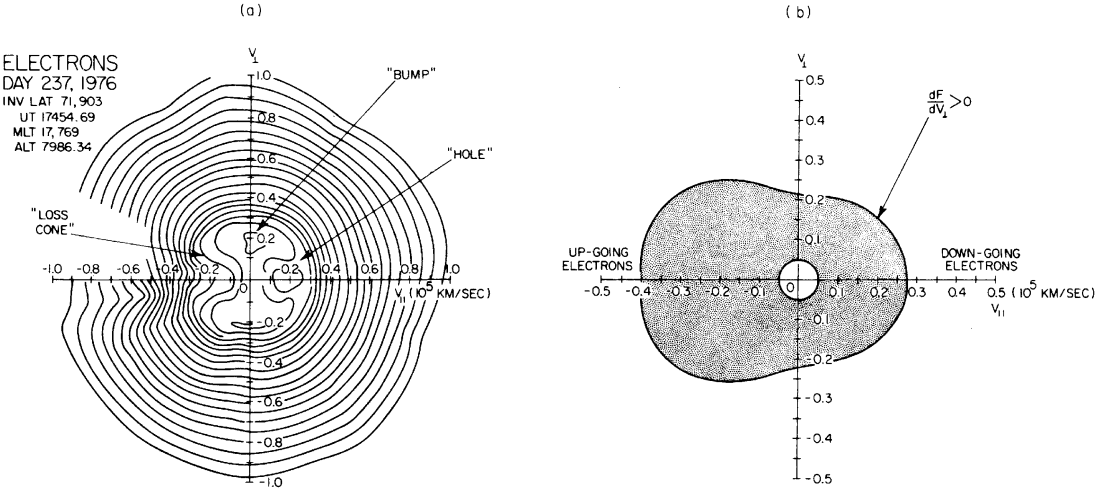

Fig. 3. The electron distribution used in calculating growth rates for AKR and Z mode radiation is shown in Figure 3*a*. The shaded area in Figure 3*b* corresponds to the region of positive $\partial F/\partial v_\perp$ in the distribution shown in Figure 3*a*. Note the different scalings in Figures 3*a* and 3*b*.

left-hand side of equation (1*b*) is negative for all $v_\parallel$ that satisfy the following condition:

$$v_\parallel > c/N_\parallel \tag{3}$$

This can be seen by noting that $v_{\parallel 0} = c/N_\parallel$ sets the left-hand side of equation (1*b*) equal to zero. It can easily be shown that the straight line $v_\parallel = c/N_\parallel$ always intersects the resonance ellipse at the perpendicular velocities

$$v_{\perp 0} = \pm c\left(1 - \frac{1}{N_\parallel{}^2}\right)^{1/2} \tag{4}$$

which correspond to $v_0 = (v_{\parallel 0}{}^2 + v_{\perp 0}{}^2)^{1/2} = c$. From equation (3) it is evident that the portion of the resonance ellipse that falls to the right of the straight line $v_\parallel = c/N_\parallel$, corresponds to false roots, i.e., particles laying on this portion of ellipse are not in resonance with waves. The nonresonance portion of the ellipse is shown in Figures 1*d*, 1*f* by broken lines.

It has been shown by *Omidi and Gurnett* [1982], *Wu et al.* [1982], *Melrose et al.* [1982], and *Dusenbery and Lyons* [1982] that for small $N_\parallel$, even with small resonance velocities the resonance ellipse does not approach the straight line $v_\parallel = c(1 - Y)/N_\parallel$ given by the nonrelativistic resonance condition

$$\omega - k_\parallel v_\parallel = n\omega_g \tag{5}$$

(rigorously speaking, the term "nonrelativistic" may not be appropriate because it is not just the velocity of the resonating electrons that determines whether equation (1) or (5) should be used but also the value of $N_\parallel$). Here, by taking the limit of large $N_\parallel$, it is shown that the resonance line (resonating portion of the ellipse) given by equation (1) approaches that of equation (5). One can see this by noting that as $N_\parallel$ gets larger the ellipse given by equation (1) becomes more eccentric, $v_{\parallel 0}$ gets smaller and $v_{\perp 0}$ approaches c. Note also that as $N_\parallel \to \infty$, the center of ellipse $V_c \to 0$, the semiminor axis $V_R \to 0$, and the semimajor axis $V_s \to c$. In Figure 2, four resonance ellipses for the Z mode corresponding to different wave normal angles are shown. It can be seen that as θ gets smaller ($N_\parallel$ becoming larger), the resonance ellipse becomes more eccentric and a smaller portion of it corresponds to resonance.

In summary, it has been shown that when the wave frequency is below the gyrofrequency (or its harmonic), both electrons with positive and negative $v_\parallel$ resonate with waves, and as we shall see in section 4, this is of great importance in the generation of the broadband Z mode radiation. It is also conceivable in the generation of the second and higher harmonics of AKR that this property of the resonance condition may play an important role [*Wu and Qiu*, 1984] by allowing waves to resonate with electrons in both the loss cone and the "hole" regions of the distribution function and also by relaxing the strict condition on f_p/f_g (f_p is the plasma frequency) ratio which is present in the generation of fundamental AKR. This can be seen by noting that for $f \sim nf_g (n \geq 2)$ the index of refraction is nearly 1, and therefore $N_\parallel \sim \cos\theta$, which means that the resonance ellipse is determined by the parameters θ and Y. It has also been demonstrated that when $N_\parallel > 1$, the particles with $v_\parallel > c/N_\parallel$ are not in resonance, and as $N_\parallel$ gets larger, the difference between the relativistic and the "nonrelativistic" resonance condition becomes less noticeable.

3. Growth Rates of AKR

In the paper by *Omidi and Gurnett* [1982], an approximate expression (equation (9)) for the imaginary part of the frequency ω_i was used to calculate growth rates of AKR. This expression was first given by *Wu and Lee* [1979] and was derived by assuming that the index of refraction was 1. Although the aforementioned equation can correctly predict the wave frequencies at which amplification or absorption take place, it fails to give an accurate rate of growth or damping, especially at frequencies near the cutoff because the effect of the plasma on the index of refraction was ignored. In order to overcome this shortcoming, we use the more accurate expression given in the appendix (equation (A5)) to calculate growth rates of AKR and Z mode radiation. This expression is obtained by including the cold plasma effects on the dispersion relation which is similar to the approach taken by *Lee and Wu* [1980]. In this section the growth rates of both the upgoing and the downgoing AKR, computed by using equation (A5), and the electron distribution measured by the S3-3 satellite are presented, and their implications in regard to the cyclotron maser instability as the amplification mechanism of

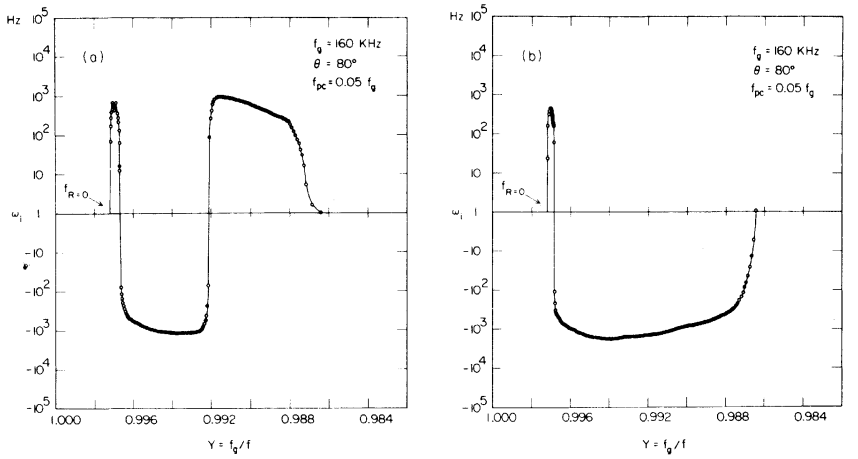

Fig. 4. Growth rates of auroral kilometric radiation for $f_{pc} = 0.05 f_g$. In Figure 4*a* waves are traveling upward, and in Figure 4*b* they are traveling downward.

the kilometric radiation are discussed. (See *Omidi and Gurnett* [1982] for the data-fitting procedure.)

Before looking at the growth rates, we find it helpful to summarize the separate sources of free energy that are commonly found in the electron distribution functions obtained by the S3-3 satellite in the auroral region. A full discussion of these distributions can be found in the work of *Croley et al.* [1978]. The first of these features is a loss cone region in the upward side of the distribution (Figure 3*a*) first suggested by *Wu and Lee* [1979] as the source of free energy in the generation of AKR. The second source of free energy is a "holelike" feature on the downward side of the distribution. Compared to the loss cone region, the "hole" is limited to smaller pitch angles and also confined to lower energy electrons. This region of the electron distribution has been pointed out by *Dusenbery and Lyons* [1982] as a possible source of free energy for the generation of the kilometric radiation. Also, in a detailed study using model distributions, *LeQueau et al.* [1984] have suggested that this source of free energy is more favorable to the amplification of AKR than the loss cone region. The third region associated with a source of free energy is a "bump" with its peak near perpendicular pitch

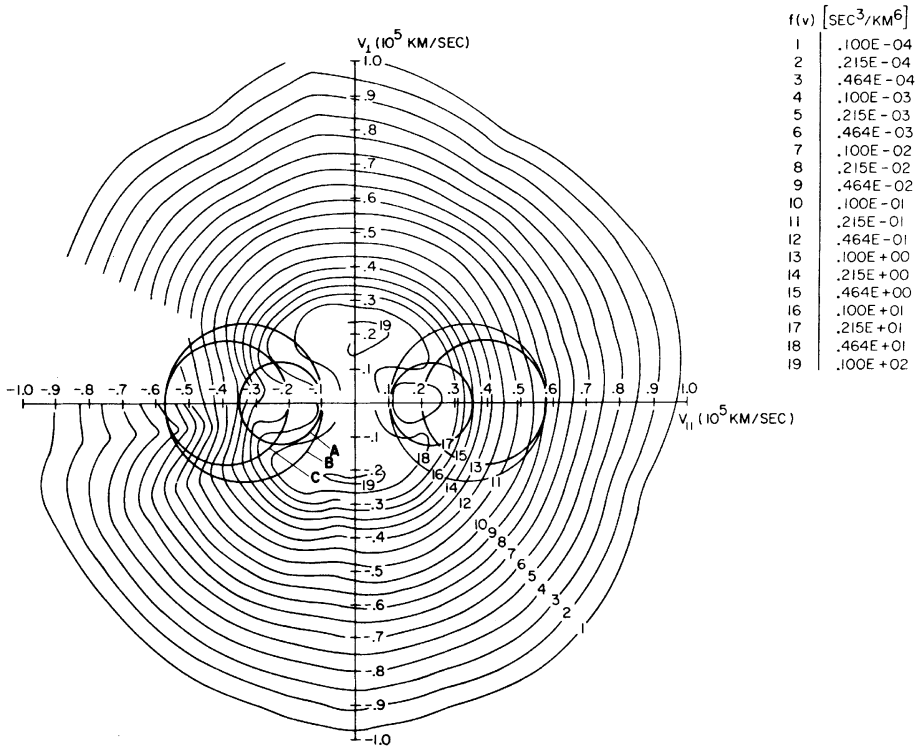

Fig. 5. Three resonance ellipses corresponding to (ellipse A) $Y = 0.997$, (ellipse B) $Y = 0.995$, and (ellipse C) $Y = 0.990$ are superimposed on both sides of the distribution. Ellipse C corresponds to growth for upgoing waves and damping for the downgoing waves.

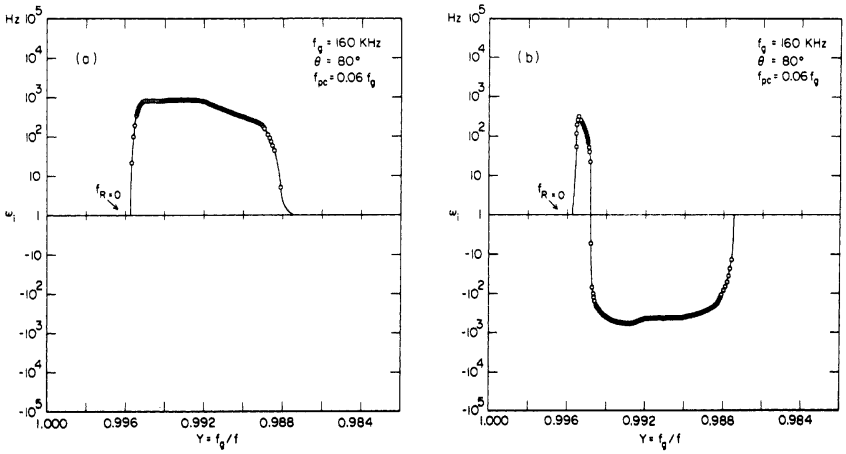

Fig. 6. Growth rates of auroral kilometric radiation for $f_{pc} = 0.06 f_g$. For upgoing waves no damping region exists, but in the case of downgoing waves a wide band corresponds to damping.

angles and energy between 0.5 and 1 keV. The presence of this bump causes the distribution function to have positive perpendicular slopes ($\partial F/\partial v_\perp$) at pitch angles near 90° and in a sense acts to bridge all three regions of free energy into almost a single continuous region of positive ($\partial F/\partial v_\perp$) at lower energies. Figure 3*b*, which shows the region of positive $\partial F/\partial v_\perp$ in a distribution function measured on day 237 of 1976, demonstrates that at low velocities perpendicular gradients are positive for almost all pitch angles, and as one goes to higher energies, positive ($\partial F/\partial v_\perp$) is limited to pitch angles away from 90°.

Since in the case of AKR (and $n = 1$) Y is always less than 1, it is clear that waves traveling in the upward direction can only resonate with the electrons in the loss cone, and the downgoing waves can only resonate with the electrons in the "hole" region. In Figure 4 the growth rates of both the upgoing and the downgoing AKR are shown for $\omega_{pc} = 0.05\omega_g$ which corresponds to a cold electron density n_c slightly larger than the warm electron density n_H, and a wave normal angle of 80°. As can be seen in Figure 4*a*, for waves traveling upward, two regions of growth and one region of damping exist. The first growth band occurs just above $f_{R=0}$ and has a peak with $\omega_i \sim 0.6$ kHz. In general, the growth rates in this region are smaller than those reported by *Omidi and Gurnett* [1982] by almost 2 orders of magnitude. This can be explained by noting that the full expression for the growth rate (equation (A5)) can after some approximations be reduced to equation (9) in the work of *Omidi and Gurnett* [1982] multiplied by the factor $\Gamma \equiv [(2\eta)/\omega(\partial/\partial\omega)\ \mathrm{Re}\ (\Lambda)]$ (see the appendix). In the first growth band $\eta \simeq 1.1$ and $\omega(\partial/\partial\omega)$ Re $(\Lambda) \simeq 150$. The growth rates obtained from equation (A5) are therefore smaller by a factor of $\Gamma = 0.015$. The second growth region starts at $Y \sim 0.992$ and ends at $Y \sim 0.987$, with corresponding values of $\eta \sim 0.159$, $\omega(\partial/\partial\omega)$ Re $(\Lambda) \sim 2.08$ and $\eta \sim 0.12$, $\omega(\partial/\partial\omega)$ Re $(\Lambda) \sim 1$, respectively, and has a peak growth rate of $\omega_i \sim 1$ kHz. From these values of η and $\omega(\partial/\partial\omega)$ Re (Λ), one can see that the growth rates in this region are on the average one fifth of the previously reported growth rates and that η plays a bigger role in reducing ω_i.

In Figure 4*b*, ω_i for the downgoing AKR is shown. In contrast to waves traveling upward, only two bands occur, a narrow growth band and a much wider damping region. One can easily explain this difference by noting that for the upgoing waves there are two frequency regions for which the reso-

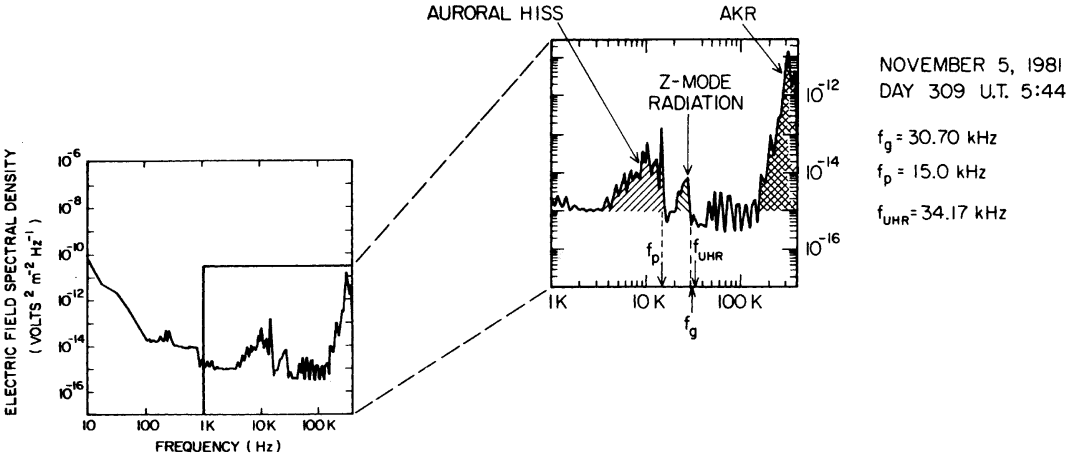

Fig. 7. An electric field spectral density corresponding to UT 0544 on day 309 of 1981. The plasma frequency is determined from the upper cutoff of the auroral hiss which propagates in the whistler mode. Note that the upper cutoff of the Z mode radiation is just below the electron gyrofrequency.

nance ellipse lies mostly or completely in the loss cone region, and thus two growth regions are obtained. However, in the case of waves traveling downward, only the resonance ellipses corresponding to frequencies near $f_{R=0}$ fall in the "hole" region, and therefore only a narrow band of frequencies above $f_{R=0}$ can be amplified (see Figure 5). Thus the fact that the free-energy region associated with the downgoing electrons is confined to smaller pitch angles and velocities makes it unlikely that this region alone can be responsible for the generation of AKR, especially since the growth rates for the downward waves are comparable to or smaller than those for the upward waves. Another argument which tends to show that it is unlikely for the "hole" region to be the primary source of free energy in the generation of AKR is that, since the growth band is very narrow and just above the cutoff frequency $f_{R=0}$, downgoing waves remain in the amplification region for only a very short time before they go through a reflection, even though the group velocity in this regime is very small. In addition, waves will not be able to maintain a large wave normal angle (which is necessary to insure resonance with electrons in the "hole") throughout their propagation in the growth region. Therefore, in the cyclotron maser theory of AKR, the loss cone region of the electron distribution seems to play a more crucial role. It should, however, be mentioned that if the laser feedback model proposed by *Calvert* [1982] is indeed an essential part of the generation mechanism of AKR, it is possible that the downgoing electrons may play an important role. In fact, it is possible that the combination of amplifications prior to and after reflection would produce a substantial growth; however, this growth would be followed by damping. Only detailed ray tracing can determine whether an overall growth is obtained or not.

In Figure 6, growth rates of AKR corresponding to $\omega_{pc} = 0.06\omega_g$ are shown. As can be seen, for waves propagating upward no region of damping exists (Figure 6*a*), since the resonance ellipses remain in the loss cone region for all frequencies. However, for the downward propagating waves a wide region of damping exists. This again demonstrates the increased importance of the upgoing electrons compared to the downgoing electrons.

Although an accurate estimate of the path length required to account for the observed intensities of AKR is obtainable only through ray tracing and path-integrated growth rates, one can find lower limits to these path lengths by assuming a constant wave normal angle θ throughout the propagation in the source region. This was done by *Omidi and Gurnett* [1982] by using an average ω_i and group velocity in each growth or damping region. By using the growth rates in Figure 4*a* and the above simple method, one finds that path lengths of 28 km and 400 km are needed for the first and second growth regions, respectively, to account for the observed intensities of AKR. Note, however, that since waves originating in the first growth region have to go through damping as they propagate upward, it is very unlikely that the first growth band can by itself be responsible for the generation of AKR, especially since the assumption of constant θ is not an appropriate one in this region. Therefore we shall only concern ourselves with the second growth band. Since in this region path lengths of more than 400 km are needed and it is unlikely that the source region is that big, one must conclude that the growth rates are not large enough to account for the direct generation of AKR. Thus if the cyclotron maser instability is to remain a viable mechanism, it is either necessary for the electron distribution in the loss cone to have a steeper slope ($\partial F/\partial v_\perp$) than those

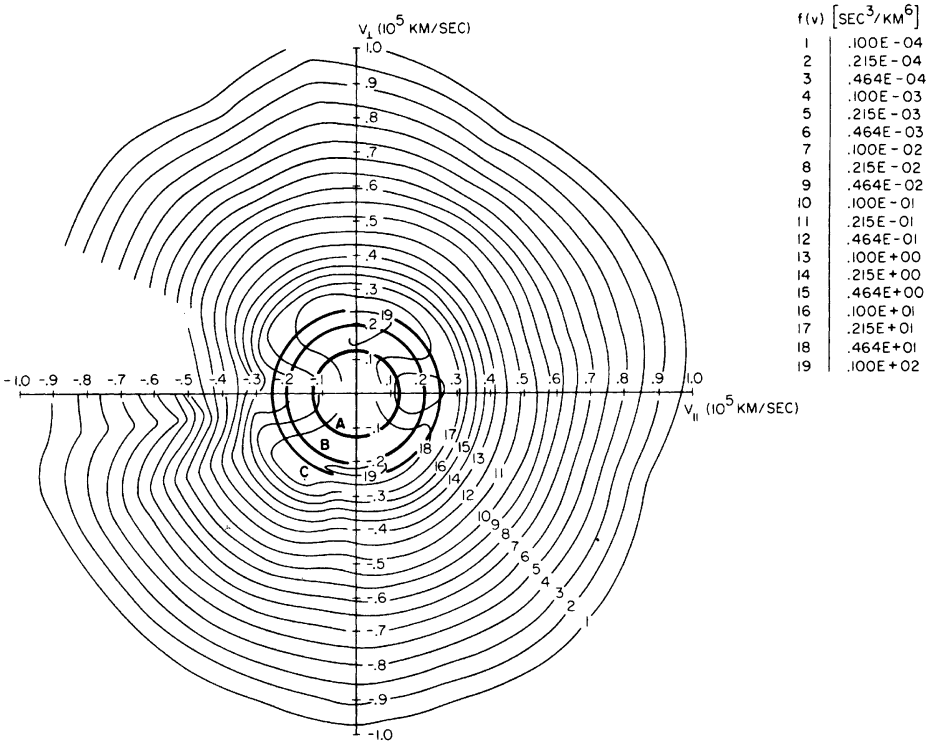

Fig. 8. Three resonance circles for Z mode corresponding to $\theta = 90°$: (ellipse A) $Y = 1.001$, (ellipse B) $Y = 1.0023$, and (ellipse C) $Y = 1.0035$ are superimposed on the electron distribution function.

measured by the S3-3 satellite, or some mechanism must exist for increasing the path length in the source region. Since interaction with the waves tends to reduce the velocity space gradients, it is possible that electron distribution functions with steeper slopes do in fact exist. However, due to the limitations imposed by the angular and temporal resolution of the S3-3 particle instrumentation, it is probably not possible that the existence of such distributions can be experimentally confirmed with existing data. A more detailed study of the theoretical limitations on the slope of the distribution function is required to see how much of an improvement can be obtained by steepening the slope at the edges of the loss cone. As previously mentioned, another possibility that could help the cyclotron loss cone instability mechanism is the laser feedback model proposed by *Calvert* [1982]. Since this model employs irregularities to reflect the waves, as in a laser, a longer effective path length can be achieved because of repeated passes of the wave through the source region. The laser feedback model reduces the requirement for growth rate to levels that appear to be reasonably consistent with the S3-3 results.

4. Growth Rates of Z Mode Radiation

In this section a summary of the recent observations of the broadband Z mode radiation by the DE 1 spacecraft is given, and the growth rates computed for this radiation based on cyclotron maser instability are presented. A full discussion of the DE 1 observations of the Z mode radiation is given by *Gurnett et al.* [1983].

As has been pointed out by *Gurnett et al.* [1983], the DE 1 measurements have identified broadband Z mode emissions in the low-density region over the auroral zone and polar cap. These measurements indicated that Z mode radiation is not observed above the local electron gyrofrequency as obtained from a model geomagnetic field. The radiation is usually most intense right below the gyrofrequency, and the intensity falls at lower frequencies. In Figure 7 an electric field intensity spectrum is shown, where the gyrofrequency is obtained from the magnetic field measured at the spacecraft (M. Sigura, unpublished data, 1983). It is clear that the upper cutoff of the Z mode radiation is indeed below the gyrofrequency, hence confirming the conclusion reached by *Gurnett et al.* [1983]. Although the Z mode radiation in a cold plasma has a cutoff at $f_{L=0} = -f_g/2 + ((f_g/2)^2 + f_p^2)^{1/2}$, where f_p is the plasma frequency, the DE 1 observations have shown that very rarely does the Z mode radiation extend from f_g all the way down to $f_{L=0}$. Furthermore, spin modulation investigations have indicated that the radiation propagates nearly or exactly perpendicular to the magnetic field. Assuming a horizontally stratified medium and a vertical magnetic field, *Gurnett et al.* [1983] have shown that these observed characteristics of the Z mode radiation can be due to propagation effects if the wave frequency in the source region is below the electron gyrofrequency. For example, an upward propagating wave generated between f_p and f_g will travel with relatively little refraction until it approaches altitudes where $f \sim f_g$, and then it will start to bend horizontally and begin to propagate nearly perpendicular to the magnetic field and asymptotically approaching an altitude where $f = f_g$.

As far as the possible source of the Z mode radiation is concerned, there has been no direct evidence from DE 1 observations indicating an exact source region [*Gurnett et al.*, 1983]. However, sometimes as the spacecraft approaches the auroral zone, the intensity of the radiation increases. In addition, observations of the auroral hiss and Z mode radiation have shown that the intensity variations of these emissions are very similar. This has led *Gurnett et al.* [1983] to conclude that the Z mode radiation is most likely generated in the same general region as the auroral hiss, however, there is no hard evidence to confirm this hypothesis. In this paper, it is hypothesized that the Z mode emissions are produced by the inverted-V electrons in the auroral zone. Since this radiation is usually observed by DE 1 at frequencies around and below 60 kHz, cyclotron resonance instability would indicate source regions at the radial distances of about 3 R_E and higher. It has been shown by *Croley et al.* [1978] that the parallel electric fields in the auroral regions extend to altitudes which are considerably higher than the S3-3 altitudes ($R \sim 2.2\ R_E$). Since features like the "bump" and the "hole" in the electron distribution used in the present calculations ($R \sim 2.2\ R_E$) are attributed to the existence of parallel electric fields, it is expected that the electron distributions at higher altitudes, where the Z mode is believed to be generated, also display these features.

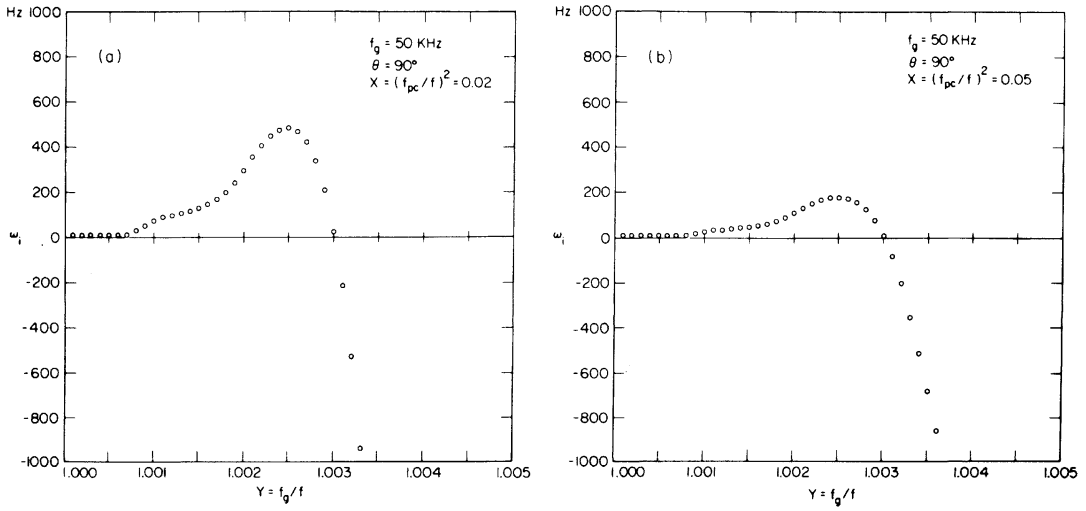

Fig. 9. Growth rates of Z mode radiation for perpendicular propagation of waves with frequencies just below the gyrofrequency. As the cold plasma density increases, ω_i decreases.

As was pointed out in section 1, all theories of the Z mode radiation have suggested that this radiation is produced by auroral electron beams; for example, *Taylor and Shawhan* [1974] have proposed incoherent Cerenkov radiation as the generation mechanism, while *Kaufman et al.* [1978] and *Maggs and Lotko* [1981] have suggested that coherent plasma instabilities are responsible for the generation of the Z mode radiation. According to these theories, generation occurs at frequencies between f_g and f_{UHR} where the Z mode is quasi-electrostatic. It has been pointed out by *Gurnett et al.* [1983] that although it is possible that the Z mode radiation may be generated between f_g and f_{UHR}, the DE 1 observations have not been able to positively confirm this. In fact, the DE 1 spacecraft has not so far detected any high-intensity quasi-electrostatic emissions near f_{UHR} in the regions where the Z mode radiation is believed to be generated. Moreover, since the Z mode is observed below the local electron gyrofrequency, one must assume the presence of horizontal density gradients to insure that waves with frequencies near f_{UHR} can propagate into regions where $f < f_g$.

In the remainder of this section it will be demonstrated that the cyclotron maser instability can explain the observed characteristics of the broadband Z mode radiation and that the calculated growth rates are large enough to account for the maximum observed intensities of this radiation.

From equations (2*a*), (2*b* and, 2*c*) it is evident that when $\theta = 90°$, the resonance ellipse becomes a circle with its center at the origin, and equation (2*c*) shows that as Y increases, the radius of this circle increases (Figure 8). In general, for θ near 90° the center of the ellipse is near the origin and its eccentricity is nearly zero. Therefore when the wave frequency f is slightly below the gyrofrequency (i.e., Y is slightly greater than 1) and θ is near 90°, the relativistic resonance condition allows waves to resonate with electrons in all three sources of free energy (in the auroral zone) mentioned in section 4, and one would expect these waves to be amplified. Results of the growth rate calculations shown in Figure 9 clearly agree with the aforementioned hypothesis and indicate that for a band of frequencies just below the gyrofrequency, relatively large growth rates are obtained. Figure 8 shows three resonance circles superimposed on the electron distribution that clearly demonstrates wave amplification when the circle simultaneously passes through the loss cone, the "hole," and the "bump" region. Waves that resonate with electrons outside of these regions are damped. Specifically, circle "C," which lies outside of the "bump" and "hole" region, gives rise to damping even though part of the circle is still within the loss cone region. In Figure 9 the growth rates corresponding to two different values of $X \equiv f_{pc}^2/f^2$ are shown which indicate that as X increases, the growth rates decrease. Note that at a given frequency this decrease is not due to a change in the resonance circle (for $\theta = 90°$ the radius is only a function of Y), but instead it is caused by the fact that as X increases, the denominator in equation (A5), $\omega(\partial/\partial\omega)$ Re (Λ), increases, and thus ω_i decreases. Therefore, just like AKR, the generation of the Z mode radiation requires a very low density region.

In Figure 10 the growth rates of both the upgoing and downgoing Z mode waves with $\theta = 85°$ are shown, which demonstrate that except for small growths for waves with frequencies just below the gyrofrequency, all waves with this wave normal angle are damped. The reason for this damping can be explained by noting that the resonance ellipses shown in Figure 11 are mostly in the regions where $\partial F/\partial v_\perp < 0$. Note that these ellipses correspond to waves traveling downward. Thus we see that as θ decreases, the center of the resonance ellipse moves away from the origin, and its radius increases. Therefore waves are not able to resonate with enough electrons with free energy to get amplified. As mentioned in section 4, it is possible that the electron distribution functions have steeper slopes ($\partial F/\partial v_\perp$) than those used in the present calculations. If this is true, the actual growth rates can be larger. Be that as it may, one can still conclude that the range of wave normal angles for which amplification is possible is rather small and near $\theta = 90°$. The reason is that as θ decreases, most or all of the resonance ellipse falls outside of free-energy source regions, and any contribution from positive ($\partial F/\partial v_\perp$) is offset by negative gradients of the distribution function.

We now wish to calculate the distances that waves have to travel in the source region before they reach the observed intensity levels. To do this it is necessary to know the group velocity v_g for $\theta = 90°$. The index of refraction for both the fast

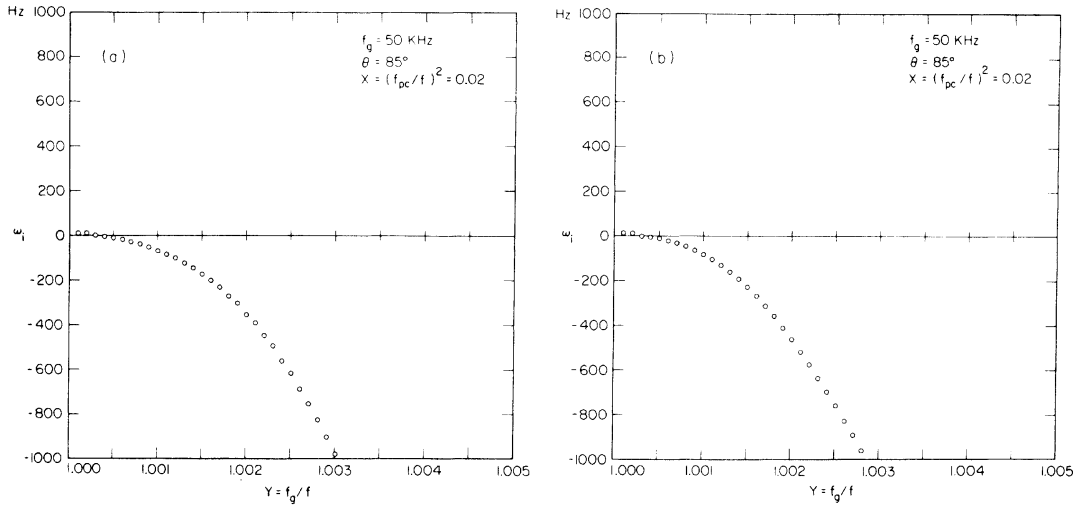

Fig. 10. Growth rates of Z mode radiation for $\theta = 85°$. Clearly, there is no significant difference between (*a*) waves propagating upward and (*b*) those traveling downward. Except for a small growth for $Y < 1.005$, all waves are damped.

and the slow extraordinary mode is given by

$$N^2 = 1 - (X/Z) \tag{6}$$

where

$$Z \equiv 1 - \frac{Y_T^2}{2(1-X)} - \left[\frac{Y_T^4}{4(1-X)^2} + Y_L^2\right]^{1/2}$$
$$Y_T \equiv Y \sin\theta \qquad Y_L = Y\cos\theta \tag{7}$$

[*Ratcliffe*, 1959]. Setting $N^2 = (c^2k^2)/\omega^2$ in equation (6) and taking derivative with $\theta = 90°$ yield the following expression for the group velocity

$$v_g\Big|_{\theta=90} = \frac{\partial\omega}{\partial k} = \frac{Nc}{1 + (XY^2)/(1 - X - Y^2)^2} \tag{8}$$

Equation (8) indicates that for $Y \sim 1$ and small X the group velocity is much less than the speed of light c, for example, $v_g \sim 0.03c$, when $Y \sim 1$ and $X \sim 0.02$. As X increases, v_g also increases, so that in order to minimize the required path lengths it is necessary to limit X to small values, especially since ω_i increases as X decreases. Note that $v_g = c$ when $X = 0$, as one would expect.

Contrary to the case of AKR where the assumption of no refraction in the source region is a poor one, it has been shown by *Gurnett et al.* [1983] that for upgoing waves with frequencies near and slightly below the gyrofrequency, the waves undergo little or no refraction. Thus the waves can travel large distances in the horizontal direction. To calculate path lengths corresponding to the growth rates in Figure 9, we assume that $\theta = 90°$ throughout the propagation in the source region. Rough estimates indicate that amplification of the background noise electric field by e^{10} is large enough to account for the maximum intensities of the Z mode radiation observed by DE 1. For these estimates the background noise has been taken to be blackbody radiation at a temperature of 3000°K, which is a typical ionospheric temperature. It is, however, expected that a stronger background noise due to Cherenkov radiation or other mechanisms exists in the source region, and thus fewer e foldings might be necessary. By using the growth rates in Figure 9 and the group velocities obtained from equation (8), we have calculated the path lengths that correspond to growth of electric fields by e^{10}. These path lengths L are shown in Figure 12. The minimum distance is $L \sim 240$ km, which is not unreasonable. Note that path lengths larger than 2000 km are not shown. It is clear from Figure 12 that as X increases, so does L. This is because at higher densities, growth rates are smaller and the group velocity is larger.

The above calculations show that waves within a narrow frequency band below the gyrofrequency grow to large amplitudes within reasonable distances. Clearly, if electron distributions with larger $(\partial F/\partial v_\perp)$ do in fact exist, then this band can be wider, and even for larger values of X (e.g., $X = 0.05$), reasonable path lengths could be obtained. Thus it is evident that the cyclotron maser instability is capable of explaining why the Z mode radiation is observed below the gyrofrequency and not between f_g and f_{UHR}. The assumption that waves with $\theta \sim 90°$ and $f \lesssim f_g$ propagate horizontally with little or no refraction is consistent with observations and allows this mechanism to amplify waves effectively. The presence of Z mode radiation at frequencies well below the gyrofrequency could also be explained by the fact that the downgoing waves with wave normal angles near 90° can continue to travel both horizontally and downward for relatively

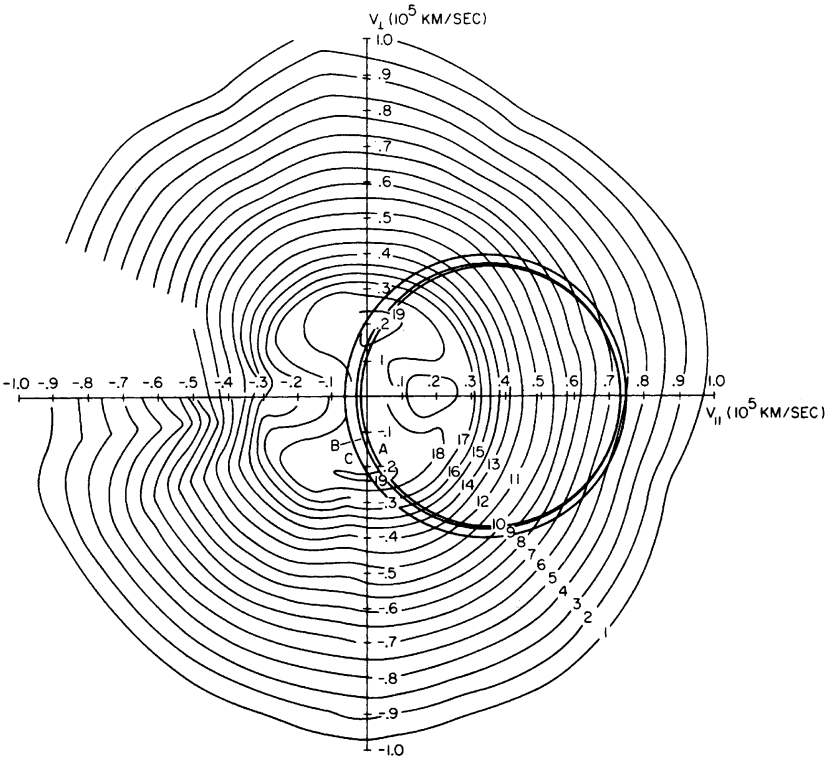

Fig. 11. Three resonance ellipses corresponding to downgoing Z mode with $\theta = 85°$: (ellipse A) $Y = 1.0005$, (ellipse B) $Y = 1.001$, and (ellipse C) $Y = 1.003$, are superimposed on the electron distribution function.

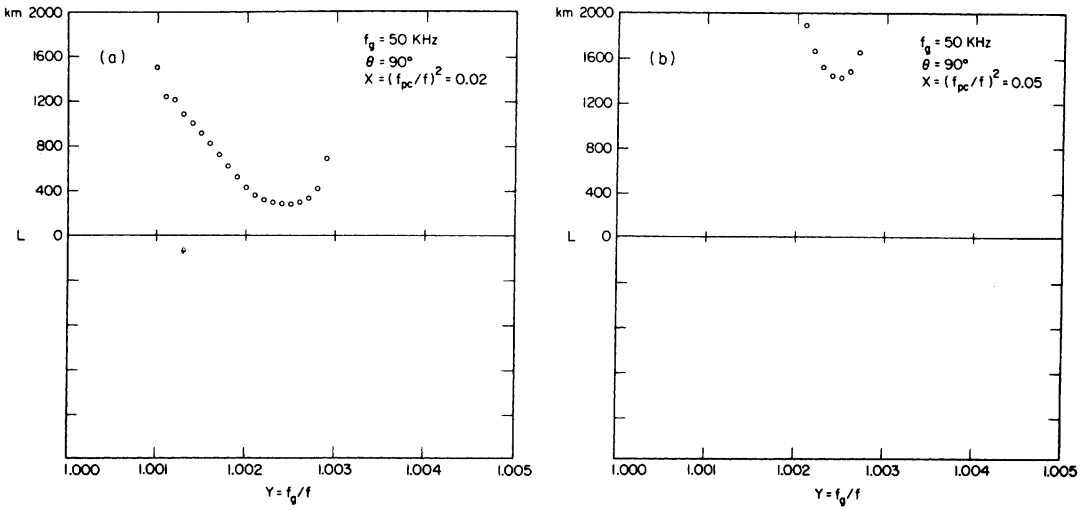

Fig. 12. The path lengths required to amplify the background blackbody radiation up to the maximum observed intensities of the Z mode radiation, using the growth rates in Figure 9.

large distances before going through reflection. Therefore at any spacecraft location it is possible to observe waves that are generated at higher altitudes. A more rigorous study through ray tracing should be performed to improve our knowledge of the ray paths and conceivably locate the source region.

Before concluding this section, it should be mentioned that occasionally, Z mode radiation is observed near $f_{L=0}$. *Gurnett et al.* [1983] have called this trapped Z mode radiation because it is trapped in the cavity formed by a local minimum in $f_{L=0}$. In this paper we have not considered the generation of these waves for which a different generation mechanism may be needed. This can be seen by noting that in order for waves to resonate with electrons in the free-energy regions of the distribution, the wave frequency must be near the local electron gyrofrequency, which means $f_{L=0} \sim f_g$. From the definition of $f_{L=0}$ it is clear that $f_{L=0} \sim f_g$ when $f_p \sim (2)^{1/2} f_g$, therefore in the low-density regions where $f_p \ll f_g$, waves with $f \sim f_{L=0}$ cannot resonate with the low-energy electrons in the free-energy regions of the distribution. It is, however, conceivable that these waves are generated in some high-density regions through the cyclotron maser instability.

5. Summary

By studying the relativistic cyclotron resonance condition, we show that the essential features of this resonance condition are determined by two parameters, Y and $N_\parallel$. When $N_\parallel \leq 1$ the resonance condition defines an ellipse in velocity space, and when $N_\parallel > 1$ only the portion of the ellipse to the left of the line $v_\parallel = c/N_\parallel$ is acceptable. It is also demonstrated that when $Y > 1$ the resonance ellipse encircles the origin, for $Y = 1$ it goes through the origin, and when $Y < 1$ it lies entirely in the region of positive parallel velocities.

By using the electron pitch angle distribution obtained by the S3-3 satellite and including the effects of cold electrons on the dispersion relation, we have calculated growth rates for both the auroral kilometric and Z mode radiation. In the case of AKR the resonance ellipse does not encircle the origin. Results of growth rate calculations show that for upgoing waves, two regions of growth exist and that these growth rates are smaller than those previously reported; on the other hand, downgoing waves can only be amplified in a narrow frequency band just above the cutoff frequency. This study seems to indicate that in the cyclotron maser theory of AKR the dominant source of free energy is most likely to be the loss cone region of the electron distribution. The magnitude of the growth rates for upgoing waves indicates minimum path lengths that are probably too large, and therefore either a laser feedback model or larger perpendicular slopes $(\partial F/\partial v_\perp)$ in the electron distribution are necessary to decrease the required path lengths.

Since the resonance ellipses corresponding to the Z mode radiation encircle the origin, it is possible for these waves to simultaneously resonate with electrons in all three sources of free energy that are commonly found in the measured distribution functions in the auroral zone. Results of growth rate calculations for the Z mode indicate that substantial growth rates are obtained when f is slightly below f_g and $\theta \sim 90°$. Assuming horizontal propagation and no refraction, the path lengths required to account for the observed intensities of the Z mode radiation were calculated, and it was shown that for a narrow frequency band near f_g, path lengths less than 400 km are obtained. These calculations suggest that the Z mode radiation may also be accounted for by the cyclotron maser theory.

Appendix: Expression for the Growth Rate

In this section, an improved expression for calculating the growth rates of AKR and Z mode radiation will be given, and the difference between this expression and the approximate equation for ω_i, first derived by *Wu and Lee* [1979] and also used by *Omidi and Gurnett* [1982] to calculate growth rates of AKR, will be discussed. The general form of the dispersion equation is

$$\Lambda = \text{determinant of } \boldsymbol{\Lambda} = 0 \tag{A1}$$

where

$$\Lambda_{ij} = N^2\left(\frac{k_i k_j}{k^2} - \delta_{ij}\right) + \varepsilon_{ij}(\mathbf{k}, \omega) \tag{A2}$$

with the dielectric tensor defined as $\varepsilon_{ij}(\mathbf{k}, \omega) \equiv \delta_{ij} + Q_{ij}(\mathbf{k}, \omega)$. The general form of $Q_{ij}(\mathbf{k}, \omega)$ is given by *Baldwin et al.* [1969] and *Lee and Wu* [1980]. In the following, we ignore the thermal effect of the higher energy electrons on the function

$\Lambda(\mathbf{k}, \omega)$ so that it can be written as

$$\Lambda = \begin{vmatrix} 1 - \dfrac{c^2 k_\parallel^2}{\omega^2} - \dfrac{\omega_{pc}^2}{\omega^2 - \omega_g^2} + i\phi & \dfrac{i\omega_{pc}^2 \omega_g}{\omega(\omega^2 - \omega_g^2)} + \phi & \dfrac{c^2 k_\parallel k_\perp}{\omega^2} - i\psi \\ -i\dfrac{\omega_{pc}^2 \omega_g}{\omega(\omega^2 - \omega_g^2)} - \phi & 1 - \dfrac{c^2 k^2}{\omega^2} - \dfrac{\omega_{pc}^2}{\omega^2 - \omega_g^2} + i\phi & \psi \\ \dfrac{c^2 k_\parallel k_\perp}{\omega^2} - i\psi & -\psi & 1 - \dfrac{c^2 k_\perp^2}{\omega^2} - \dfrac{\omega_{pc}^2}{\omega^2} \end{vmatrix} = 0 \tag{A3}$$

where the imaginary part of Q_{zz} has been set equal to zero; $k_\parallel$ and $k_\perp$ are the components of $\mathbf{k}$ parallel and perpendicular to the magnetic field, respectively, and

$$\phi = -2\pi^2 \frac{\omega_{PH}^2}{\omega} \cdot \int_{-\infty}^{\infty} du_\parallel \int_0^{\infty} du_\perp \left[\frac{\partial}{\partial u_\perp} + \frac{k_\parallel}{\gamma\omega}\left(u_\perp \frac{\partial}{\partial u_\parallel} - u_\parallel \frac{\partial}{\partial u_\perp}\right)\right] \cdot F_e \frac{u_\perp^2}{4} \delta(\gamma\omega - \omega_g - k_\parallel u_\parallel) \tag{A4}$$

$$\psi = +2\pi^2 \frac{\omega_{PH}^2}{\omega} \int_{-\infty}^{\infty} du_\parallel \cdot \int_0^{\infty} \cdot du_\perp \left[\frac{\partial}{\partial u_\perp} + \frac{k_\parallel}{\gamma\omega}\left(u_\perp \frac{\partial}{\partial u_\parallel} - u_\parallel \frac{\partial}{\partial u_\perp}\right)\right] \cdot F_e \frac{k_\perp u_\perp^2 u_\parallel}{4\omega_g} \delta(\gamma\omega - \omega_g - k_\parallel u_\parallel)$$

with F_e being the unperturbed distribution of electrons normalized to unity, ω_{pc} and ω_{PH} being the angular plasma frequency of the cold and warm electrons, respectively, $u_\parallel$ and $u_\perp$ being electron momentum per unit mass parallel and perpendicular to the magnetic field, and $\gamma \equiv (1 + u^2/c^2)^{1/2}$.

Equation (A3) consists of a real part and an imaginary part. The real part of equation (A3) will give the relation between ω (real part of frequency) and $\mathbf{k}$, and since thermal effects were ignored in obtaining Re $\{\Lambda(\mathbf{k}, \omega)\}$, the resulting index of refraction is the same as that in a cold plasma discussed by *Stix* [1962]. The expression for the growth rate ω_i is then given by

$$\frac{\omega_i}{\omega} = -\frac{\text{Im } (\Lambda)}{\omega(\partial/\partial\omega) \text{ Re } (\Lambda)} \tag{A5}$$

where the imaginary part of Λ is

$$\text{Im } (\Lambda) = \eta\phi + \rho\psi \tag{A6}$$

with η and ρ defined as

$$\eta \equiv \left[2 - \frac{c^2}{\omega^2}(k^2 + k_\parallel^2) - \frac{2\omega_{pc}^2}{\omega(\omega + \omega_g)}\right]\left(1 - \frac{c^2 k_\perp^2}{\omega^2} - \frac{\omega_{pc}^2}{\omega^2}\right) - c^4 \frac{k_\parallel^2 k_\perp^2}{\omega^4} \tag{A7}$$

$$\rho \equiv 2\frac{c^2 k_\parallel k_\perp}{\omega^2}\left(1 - \frac{c^2 k^2}{\omega^2} - \frac{\omega_{pc}^2}{\omega(\omega + \omega_g)}\right)$$

The term in the denominator of equation (A5) can be expressed as

$$\omega \frac{\partial}{\partial\omega} \text{Re } (\Lambda) = 2N^4\left[\frac{\omega^2\omega_{pc}^2 \sin^2\theta}{(\omega^2 - \omega_g^2)^2} + \frac{\omega_{pc}^2 \cos^2\theta}{\omega^2}\right] + 4N^2\left[\frac{\omega_{pc}^2(\omega_{pc}^2 - \omega_g^2)}{(\omega^2 - \omega_g^2)^2} - 1 - \frac{\omega_{pc}^2\omega_g^2 \sin^2\theta}{2(\omega^2 - \omega_g^2)^2}\right] + 2\left[\left(2 - \frac{\omega_{pc}^2}{\omega^2}\right)\left(1 - \frac{\omega_{pc}^2}{\omega^2 - \omega_g^2}\right)^2 - \frac{\omega_{pc}^4\omega_g^2}{\omega^2(\omega^2 - \omega_g^2)^2} + 2\left(1 - \frac{\omega_{pc}^2}{\omega^2}\right)^2 \frac{\omega^2\omega_{pc}^2}{(\omega^2 - \omega_g^2)^2}\right] \tag{A8}$$

Although it was shown by *Lee and Wu* [1980] that, in comparison with the results of *Wu and Lee* [1979], smaller growth rates are obtained when the effects of cold electrons are included in the dispersion relation, it is instructive to see how equation (A5) can be reduced to the expression for ω_i given by *Wu and Lee* [1979]. In order to do this, it is necessary to transform ϕ and ψ from momentum space into velocity space. Upon this transformation ϕ and ψ are given by

$$\phi = -\frac{\pi^2}{2}\frac{\omega_{PH}^2}{\omega^2} \int_{-\infty}^{\infty} dv_\parallel \int_0^{\infty} dv_\perp v_\perp^2 \left[\omega_g \frac{\partial F_e}{\partial v_\perp} + k_\parallel v_\perp \frac{\partial F_e}{\partial v_\parallel}\right] \cdot \delta\left(\omega - \frac{\omega_g}{\gamma_v} - k_\parallel v_\parallel\right) \tag{A9}$$

$$\psi = \frac{\pi^2}{2}\frac{\omega_{PH}^2}{\omega^2} \int_{-\infty}^{\infty} dv_\parallel \int_0^{\infty} dv_\perp \frac{k_\perp v_\parallel v_\perp^2}{\omega_g} \left[\omega_g \frac{\partial F_e}{\partial v_\perp} + k_\parallel v_\perp \frac{\partial F_e}{\partial v_\parallel}\right] \cdot \delta\left(\omega - \frac{\omega_g}{\gamma_v} - K_\parallel v_\parallel\right)$$

where $\gamma_v \equiv (1 - v^2/c^2)^{-1/2}$ has been set equal to one everywhere except in the delta function; and terms like $v_\parallel v_\perp/c^2$ and $v_\perp^2/c^2$ have been dropped. From equation (A9) one can see that the integrand of ψ is that of ϕ times the factor $(k_\perp v_\parallel/\omega_g)$. Since in the case of *R-X* mode for $\omega \sim \omega_g \gg \omega_p$, η is greater than ρ, for small $v_\parallel/c$ the second term in equation (A6) can be dropped and equation (A5) can be rewritten as

$$\omega_i = (2\eta)\left[\frac{\pi^2\omega_{PH}^2}{4\omega} \int_{-\infty}^{\infty} dv_\parallel \int_0^{\infty} dv_\perp v_\perp^2 \left(\omega_g \frac{\partial F_e}{\partial v_\perp} + k_\parallel v_\perp \frac{\partial F_e}{\partial v_\parallel}\right) \cdot \delta\left(\omega - \frac{\omega_g}{\gamma_v} - k_\parallel v_\parallel\right)\right] \Big/ \left(\omega \frac{\partial}{\partial\omega} \text{Re } (\Lambda)\right) \tag{A10}$$

Since the expression in the bracket in the numerator is just equation (9) (for ω_i) in the work of *Omidi and Gurnett* [1982], it is evident that the reported growth rates are nearly off by a factor of $(2\eta)/(\omega(\partial/\partial\omega) \text{ Re } (\Lambda))$. As is shown in section 3, at frequencies near the cutoff ($f_{R=0}$) $\eta > 1$, and therefore it is the denominator of the above factor that will cause the reduction of the previously reported growth rates, while at higher frequencies η is less than 1, and it too will cause a reduction in the reported growth rates of AKR.

Acknowledgments. The authors wish to thank M. Sigura for providing them with magnetic field measurements and R. Huff for making the electric field intensity spectrum available. The research at

the University of Iowa was supported by the National Aeronautics and Space Administration through grants NGL-16-001-043 and NGL-16-001-002 with NASA Headquarters, and by grant NAS5-26819 with NASA Goddard Space Flight Center. The research at the University of Maryland was supported by NASA under grant NGL-21-002-005.

The Editor thanks A. Roux and D. B. Melrose for their assistance in evaluating this paper.

REFERENCES

Baldwin, D. E., I. B. Bernstein, and M. P. H. Weenink, *Advances in Plasma Physics*, vol. 3, John Wiley, New York, 1969.

Benson, R., and W. Calvert, ISIS 1 observations at the source of auroral kilometric radiation, *Geophys. Res. Lett.*, 479, 1979.

Calvert, W., A feedback model for the source of auroral kilometric radiation, *J. Geophys. Res.*, *87*, 8199, 1982.

Croley, D. R., P. F. Mizera, and J. F. Fennel, Signature of a parallel electric field in ion and electron distributions in velocity space, *J. Geophys. Res.*, *83*, 2701, 1978.

Dusenbery, P. B., and L. R. Lyons, General concepts on the generation of auroral kilometric radiation, *J. Geophys. Res.*, *87*, 7467, 1982.

Green, J. L., D. A. Gurnett, and R. A. Hoffman, A correlation between auroral kilometric radiation and inverted-V electron precipitation, *J. Geophys. Res.*, *84*, 5216, 1979.

Gurnett, D. A., The earth as a radio source: Terrestrial kilometric radiation, *J. Geophys. Res.*, *83*, 689, 1978.

Gurnett, D. A., and J. L. Green, On the polarization and origin of auroral kilometric radiation, *J. Geophys. Res.*, *83*, 689, 1978.

Gurnett, D. A., S. D. Shawhan, and R. R. Shaw, Auroral hiss, *Z* mode radiation and auroral kilometric radiation in the polar magnetosphere: DE 1 observations, *J. Geophys. Res.*, *88*, 329, 1983.

Hewitt, R. G., D. B. Melrose, and K. G. Rönnmark, The loss-cone driven electron-cyclotron maser, *Aust. J. Phys.*, *35*, 447, 1982.

Kaiser, M. L., and R. G. Stone, Earth as an intense planetary radio source: Similarities to Jupiter and Saturn, *Science*, *189*, 285, 1975.

Kaiser, M. L., J. K. Alexander, A. C. Riddle, J. B. Pearce, and J. W. Warwick, Direct measurements of the polarization of terrestrial kilometric radiation from Voyagers 1 and 2, *Geophys. Res. Lett.*, *5*, 857, 1978.

Kaufman, R. L., P. B. Dusenbery, and B. J. Thomas, Stability of the auroral plasma: Parallel and perpendicular propagation of electrostatic waves, *J. Geophys. Res.*, *83*, 5663, 1978.

Kurth, W. S., M. M. Baumback, and D. A. Gurnett, Direction-finding measurements of auroral kilometric radiation, *J. Geophys. Res.*, *80*, 2764, 1975.

Lee, L. C., and C. S. Wu, Amplification of radiation near cyclotron frequency due to electron population inversion, *Phys. Fluids*, *23*, 1348, 1980.

LeQueau, D., R. Pellat, and A. Roux, Direct generation of the auroral kilometric radiation by the maser synchrotron instability: An analytic approach, *Phys. Fluids*, in press, 1984.

Maggs, J. E., and W. Lotko, Amplification of electrostatic noise in cyclotron resonance with an adiabatic auroral beam, *J. Geophys. Res.*, *86*, 3449, 1981.

Melrose, D. B., An interpretation of Jupiter's radiation and the terrestrial kilometric radiation as direct amplified gyroemission, *Astrophys. J.*, *207*, 651, 1976.

Melrose, D. B., K. G. Rönnmark, and R. G. Hewitt, Terrestrial kilometric radiation: The cyclotron theory, *J. Geophys. Res.*, *87*, 5140, 1982.

Omidi, N., and D. A. Gurnett, Growth rate calculations of auroral kilometric radiation using the relativistic resonance condition, *J. Geophys. Res.*, *87*, 2377, 1982.

Ratcliffe, J. A., *The Magneto-Ionic Theory and Its Applications to the Ionosphere*, Cambridge University Press, New York, 1959.

Shawhan, S. D., and D. A. Gurnett, The polarization of auroral kilometric radiation, *Geophys. Res. Lett.*, *9*, 913, 1982.

Stix, T. H., *The Theory of Plasma Waves*, McGraw-Hill, New York, 1962.

Taylor, W. W. L., and S. D. Shawhan, A test of incoherent Cerenkov radiation for VLF hiss and other magnetospheric emissions, *J. Geophys. Res.*, *79*, 105, 1974.

Wu, C. S., and L. C. Lee, A theory of the terrestrial kilometric radiation, *Astrophys. J.*, *230*, 621, 1979.

Wu, C. S., and X. M. Qiu, Emissions of second harmonic auroral kilometric radiation, *J. Geophys. Res.*, in press, 1984.

Wu, C. S., H. K. Wong, D. J. Gorney, and L. C. Lee, Generation of the auroral kilometric radiation, *J. Geophys. Res.*, *87*, 4476, 1982.

D. A. Gurnett and N. Omidi, Department of Physics and Astronomy, University of Iowa, Iowa City, IA 52242.

C. S. Wu, Institute for Physical Science and Technology, University of Maryland, College Park, MD 20742.

(Received May 19, 1983;
revised September 12, 1983;
accepted October 14, 1983.)